Schisandrin A protects intestinal cells from mycophenolic acid-induced cytotoxicity and oxidative damage

Yiyun Deng
Anhui Medical University
Zhe Zhang
Anhui Medical University
Yuanyuan Hong
Anhui Medical University
Lijuan Feng
The First Affiliated Hospital of Anhui Medical University
Yong Su
The First Affiliated Hospital of Anhui Medical University
Dujuan Xu (xudujuan2011@163.com)
The First Affiliated Hospital of Anhui Medical University https://orcid.org/0000-0001-5743-3876

Research Article

Keywords: Mycophenolic acid (MPA), Schisandrin A (Sch A), Tight junction proteins (TJs), oxidative stress, mitogen-activated protein kinases (MAPK)

Posted Date: August 6th, 2021

DOI: https://doi.org/10.21203/rs.3.rs-767385/v1

Abstract

Objectives: The gastrointestinal side effects of mycophenolic acid affect its efficacy in kidney transplant patients, which may be due to its toxicity to the intestinal epithelial mechanical barrier, including intestinal epithelial cell apoptosis and destruction of tight junctions. The toxicity mechanism of mycophenolic acid is related to oxidative stress-mediated the activation of mitogen-activated protein kinases (MAP K). Schisandrin A (Sch A), one of the main active components of the Schisandra chinensis, can protects intestinal epithelial cells from deoxynivalenol-induced cytotoxicity and oxidative damage by antioxidant effects. The aim of this study was to investigate the protective effect and potential mechanism of Sch A on mycophenolic acid-induced damage in intestinal epithelial cell. Methods: Caco-2 cells monolayers were treated with mycophenolic acid (10μM) and/or Sch A (10, 20 and 40μM) at 37°C for 24h, and cell viability was measured by MTT; Western blot and immunofluorescence were used to detect the expression of relevant proteins. Intracellular ROS and apoptosis were measured by flow cytometry, and malondialdehyde (MDA) and superoxide dismutase (SOD) levels were measured by kits. Results: The results showed that Sch A significantly reversed the mycophenolic acid-induced cell viability reduction, restored the expression of tight junction protein ZO-1, occludin and reduced cell apoptosis. In addition, Sch A inhibited mycophenolic acid-mediated MAPK activation and reactive oxygen species (ROS) increase. Conclusions: Sch A protected intestinal epithelial cells from mycophenolic acid intestinal toxicity, at least in part, by reducing oxidative stress and inhibiting MAPK signaling pathway. Conclusions: Sch A protected intestinal epithelial cells from mycophenolic acid intestinal toxicity, at least in part, by reducing oxidative stress and inhibiting MAPK signaling pathway.

Introduction

Mycophenolic acid (MPA) is an immunosuppressant commonly used as adjuvant therapy in kidney transplantation, which can effectively improve the long-term survival rate of the graft, but also has many adverse reactions [1]. Gastrointestinal adverse reactions such as vomiting and diarrhea are one of the most common adverse reactions [2]. The patients with gastrointestinal adverse reactions have to reduce the dose or even stop mycophenolic acid treatment, which lead to an increased risk of rejection and affect the outcome of the transplantation [3, 4].

The intestinal toxicity of mycophenolic acid is related to the damage of the intestinal mechanical barrier, which is composed of intestinal epithelial cells and tight junctions between the cells [5]. Increased apoptosis of intestinal epithelial cells and altered expression of paracellular tight junction proteins (TJs) may both lead to mechanical barrier defects and cause intestinal symptoms such as diarrhea, gastrointestinal bleeding and enteritis [6, 7]. TJs are important components of the intestinal epithelial barrier, which located at the most apical part of the epithelium, and consist mainly of transmembrane proteins (e.g., occludin, claudins) and peripheral proteins (e.g., ZO-1) [8]. Previous reports have shown that mycophenolic acid disrupts the intestinal mechanical barrier by altering the expression of TJs through activation ERK/p38/MLCK pathway [9, 10]. Moreover, activated mitogen-activated protein kinases (MAPK) induces apoptosis by increasing Caspase 3 cleavage and Bax expression in intestinal cells [11].

It has been confirmed that activation of the MAPK signaling pathway in intestinal epithelial cells is related to the redox state of the cells. Oxidative stress-mediated increase in reactive oxygen species (ROS) can directly activate the MAPK [12]. MPA can cause dose-dependent mitochondrial dysfunction and increase the production of ROS [13]. Therefore, inhibition of MAPK activation regulated by oxidative stress may be a therapeutic target to alleviate the intestinal toxicity of MPA.

Our group's previous clinical observation found that diarrhea was significantly improved in patients who took mycophenolate mofetil (MMF) (a pre-MPA drug) in combination with WuZhi capsules. The main ingredient of WuZhi capsules is Schisandrin A (Sch A). Sch A is one of the main active components of Schisandra chinensis (turcz.) baill of the Magnoliaceae family, with various pharmacological effects such as antioxidant [14, 15]. In addition, Sch A protects intestinal epithelial cells from deoxynivalenol-induced oxidative damage in human colon cancer HT-29 cells by inhibiting MAPK signaling pathway [16].

Therefore, we hypothesized that Sch A could alleviate MPA-induced apoptosis and TJs expression reduction in intestinal epithelial cells through inhibiting oxidative stress-mediated activation of the MAPK. In the present study, we explored the protective effect and mechanism of Sch A on MPA-induced intestinal cell damage in Caco-2 cell.

Materials And Methods

Chemicals and Reagents

Sch A (purity ≥ 98%) was purchased from Solarbio Biotechnology Co., Ltd (Beijing, China). MPA (purity ≥ 98%) was purchased from Yuanye Biological Technology Co., Ltd (Shanghai, China). Specific antibodies were purchased from different companies as follows: GAPDH (1:10000; ab181602, Abcam, UK); Bax (1:1000; ab32503, Abcam, UK); ZO-1, Caspase-3 (1:1000; #AF5145, #DF6879, Affinity Bioscience, China), p-ERK, P38, p-P38, JNK, p-JNK (1:500; sc-7383, sc-7972, sc-166182, sc-7345, sc-6254, Santa Cruz Biotechnology, USA), ERK (1:1000; 4695S, Cell Signaling Technology, USA), and Bcl-2, occludin (1:1000; 383309, 502601, ZENBio, China).

Cell culture

The human colon adenocarcinoma cell line Caco-2 was kindly provided by Dr. Shuai Song (The First Affiliated Hospital of Anhui Medical University, China). Cells were routinely cultured in complete Dulbecco's modified Eagle's medium (DMEM) (4.5 g/L glucose) (Gibco, MD, USA) with 10% fetal bovine serum (Gibco, MD, USA) and 1% streptomycin (100 μg/mL)/penicillin (100U/ mL) at 37 °C with 5% CO2.

Western blotting

Cells were lysed with RIPA lysis buffer containing 1% protease inhibitor (Beyotime Biotechnology, China). Protein samples were loaded and separated by 10% or 12% SDS-PAGE and transferred to polyvinylidene fluoride membranes (Millipore, Bedford, MA, USA). The membranes were then blocked with 5% nonfat dry

milk in TBST (10 mM Tris, 150 mM NaCl, and 0.1% Tween 20) buffer for 1h at room temperature. Then the membranes were washed three times with 0.1% T-TBS and each membrane was incubated with primary antibodies overnight at 4 °C. After washing with TBST the next day, the membranes were probed with the appropriate secondary peroxidase-conjugated antibody (ZSGBbio, China) for 1 h at room temperature. For all gels, GAPDH was used as the internal standard. The membranes were detected by electrochemiluminescence (Applygen Technologies, Inc. China). Protein bands were quantified and normalized with Image J software.

Cell viability assay

A density of 4×10^3 cells seeded in 96-well plates with complete medium. Every other day, the cells were treated with different concentrations MPA and Sch A for 24 h or 48 h, then assessed for viability by the methyl thiazolyl tetrazolium (MTT) assay. The absorbance was assessed at 490 nm with a microplate spectrophotometer (Bio-Tek, USA). All experiments were repeated at least three times.

Immunofluorescence

The cells were seeded on a 24-well plate. After treating the cells with different concentrations of MPA and Sch A for 24 h, the cells were washed with PBS and fixed in 4% formaldehyde at room temperature for 15 min. It was then rinsed in PBS and permeabilized in 0.5% Triton X-100 for 10 min at room temperature. The cells were rinsed in PBS and then blocked with 1% bovine serum albumin for 30 min at 37 °C. After rinsing with PBS, the cells were incubated overnight with ZO-1 antibody (1:250; Affinity Bioscience, China), occludin antibody (1:100; ZENBio, China) at 4 °C. Then, the secondary antibody was incubated for 1 h in the dark at room temperature. 4', 6 diamine phenlinone (DAPI) was used for nuclear staining. The fluorescence was visualized using a confocal microscope (Zeiss, Germany).

Intracellular reactive oxygen species (ROS) measurement

ROS was measured using a flow cytometry (Beckman Coulter, Brea, CA, USA) and a fluorescence inverted microscope (Olympus Corporation, Japan). Cells were seeded and cultured in 6-well or 24-well plates to 90% confluence, as mentioned before, treated them with MPA and Sch A. The cells for flow cytometry were digested the adherent cells with trypsin to prepare a viable cell suspension (10^6 cells/mL). Treated with 1 ml of H_2DCFDA working solution (H_2DCFDA stock solution was diluted with PBS to prepare 5 μM) (KeyGEN BioTECH, China) at 37 °C for 20 min. Then, washed the cells twice with PBS, and immediately detected with flow cytometry or fluorescence inverted microscope.

Superoxide dismutase (SOD) activity analysis and malondialdehyde (MDA) content determination

Caco-2 cells in logarithmic growth phase were inoculated into cell culture flasks, fused and grown for one week, and treated with drugs for 24 h as described above. Washed three times with PBS, added lysate to collect cells, centrifuged at 1000r for 10 min to get the supernatant. BCA protein quantification kit (Beyotime Biotech, China) was used to detect protein content, and the final treatment solution was added

to 96-well plates according to the instructions of SOD and MDA assay kit (Jiancheng Bioengineering Institute, China), and the absorbance was detected at wavelengths of 450 nm or 530 nm. Then calculated SOD activity and MDA content according to the calculation formula.

Apoptosis Analysis

After the cell culture was completed, the cells were digested without EDTA, and the cells in the culture medium were collected. Centrifuge at 300g for 5 min in a centrifuge. Discarded the supernatant, added PBS to resuspend and centrifuge, repeated 2 times. Resuspended the cells with 400 μL of AnnexinV binding solution, added 4 μL of AnnexinV-FITC in the dark, and incubated for 15 min in the dark. Then added 7.5 μL of PI staining solution, mixed gently, incubated in the dark for 5 min, and then tested in the flow cytometer.

Statistical analysis

All data were statistically analyzed using Statistical Program for Social Sciences v.26.0 software (SPSS Inc., Chicago, IL, USA). The data was normally distributed and expressed by the mean standard deviation (SD). The difference analysis was carried out by one-way (ANOVA). All experiments were repeated at least three times. $P < 0.05$ was considered statistically significant.

Results

Sch A protects against MPA-induced cytotoxicity in Caco-2 cells

In order to determine the concentration of MPA and Sch A used in the follow-up study, we treated Caco-2 cells with different concentrations of MPA and Sch A, and measured the viability of the treated cells through the MTT experiment. Compared with the control group, all experimental concentrations of MPA resulted in a significant decrease in cell viability ($P < 0.05$) (Fig. 1a), while Sch A decreased cell viability above 50 μM (Fig. 1b). Therefore, the intermediate concentration of MPA was 10 μM and the maximum concentration of Sch A was 50 μM for subsequent experiments. In order to test the protective effect of Sch A on MPA-induced cytotoxicity, Caco-2 cells were treated with 10 μM MPA and different concentrations of Sch A for 24 h or 48 h. Our results showed that Sch A (10-50 μM) significantly attenuated the decrease in cell viability caused by 10 μM MPA in a time- and dose-dependent manner (Fig. 1c).

Sch A reverses MPA-induced down-regulation of occludin and ZO-1 protein expression in Caco-2 cells

Tight junctions (TJs) are critical to the integrity of the intestinal epithelial barrier. Previous studies have shown that MPA damages intestinal epithelial cells because it impairs the expression and distribution of TJs proteins [17]. Therefore, we tested the expression and distribution of two representative TJs proteins, ZO-1 and occludin in Caco-2 cell monolayer treated with Sch A and/or MPA. As shown in Fig. 2a, the results of Western blot showed that the expression of occludin and ZO-1 in Caco2 cells treated with MPA for 24h was significantly reduced compared with the control group, while after cotreatment with Sch A for

24h, the expression of ZO-1 and occludin increased in a dose-dependent manner. Similar results were obtained from immunofluorescence experiments. Sch A treatment can partially prevent the redistribution of ZO-1 and occludin induced by MPA and re-close the paracellular space. Overall, these data indicate that Sch A effectively protects the TJs of the intestinal epithelium damaged by MPA (Fig. 2b).

Sch A reduces MPA-induced apoptosis in Caco-2 cells

MPA has been reported to be related to the apoptosis of intestinal epithelial cells, so we detected the expression of apoptosis-related proteins. As shown in Fig. 3a, there was no significant change in the expression of the pro-apoptotic protein Bax, but compared with the control group, MPA reduced the expression of the anti-apoptotic protein Bcl-2 ($P < 0.05$). After treatment with Sch A for 24 h, MPA-induced apoptosis was significantly reduced by up-regulating Bcl-2 ($P < 0.05$ or $P < 0.01$). In addition, MPA increased the activation of Caspase-3, while Sch A inhibited the activation of Caspase-3 ($P < 0.01$). Subsequently, in order to further confirm whether the reduction of apoptosis is related to the protective effect of Sch A, we used Annexin V-FITC/PI staining to measure apoptosis. As shown in Fig. 3b and 3c, MPA significantly increased the early and late apoptosis rates of Caco-2 cells and reduced the percentage of normal cells ($P < 0.05$), and Sch A reversed the up-regulation of MPA on the apoptosis rate and increased the percentage of normal cells ($P < 0.05$).

Sch A inhibits MPA-induced activation of MAPK signaling pathway

To further explore the molecular signaling pathway of the protective effect of Sch A in the intestine, the effect of Sch A on ERK/JNK/p38 MAPK pathway in the MPA model was investigated by Western blot (Fig. 4).

Sch A reduces oxidative stress induced by MPA in Caco-2 cells

The imbalance between oxidation and antioxidant systems causes increased accumulation of ROS, oxidative stress, and oxidative damage to cells. In order to test whether Sch A reduces the oxidative stress induced by MPA in Caco-2 cells, firstly, we detected the production of ROS. The results of flow cytometry and H_2DCFDA staining experiments showed that after MPA treatment, the ROS level in Caco-2 cells was significantly higher than that in control cells, while Sch A and MPA co-treatment significantly reduced ROS in cells ($P < 0.05$) (Fig. 5a-c). Next, we tested the activity of SOD and the content of MDA. As shown in Fig. 5d-e, compared with the MPA group, Sch A significantly increased SOD activity and reduced MDA content ($P < 0.05$).

Discussion

MPA is commonly used as an immunosuppressive agent in adjuvant renal transplantation, which effectively improves long-term graft survival, but the accompanying gastrointestinal adverse effects such as diarrhea greatly limit its use. It is now generally accepted that diarrhea caused by MPA may be due to damage to intestinal epithelial cells [18]. Our results suggest that Sch A can act as a protective agent

against MPA-induced Caco-2 cell injury. The results of MTT assay showed that 10–50 μM of Sch A protected cells from MPA-induced cell damage and partially reversed the inhibition of cell viability by MPA. Therefore, this concentration range was selected for subsequent experiments.

The intestinal barrier includes three types of barriers: biological barrier, immune barrier and mechanical barrier. Mechanical barriers are important in maintaining intestinal function, which is a tight structure established by epithelial and endothelial cells interconnected through a tight junction (TJ) structure. Mechanical barriers effectively restrict the passage of bacteria and endotoxins [19, 20]. Both increased apoptosis of intestinal epithelial cells and altered expression of paracellular tight junction proteins may lead to mechanical barrier defects in the intestinal epithelium, resulting in intestinal barrier dysfunction and causing diarrhea and enteritis [21]. “Tight junction” is an apical junctional complex (AJC) which consists of a variety of tight junction protein (TJs). It is reported that deletion of TJs induces increased paracellular permeability in vivo and in vitro, which in turn leads to diarrhea [22]. ZO-1 is an early identified cytoplasmic peripheral membrane protein of TJs, which consists of an amino-terminal and a carboxy-terminal half. Occludin is a transmembrane protein that binds to the amino-terminal of ZO-1 to form a tight junction complex. The carboxy-terminal of ZO-1 anchors this complex to the cytoskeleton by binding F-actin (cytoskeletal protein), which forms the paracellular barrier [23]. Our study showed that Sch A upregulated the expression of ZO-1 and occludin, and reduced the gap between intestinal epithelial cells.

In addition, apoptosis is one of the manifestations of MPA-induced intestinal epithelial cell damage [24, 25]. A certain degree of apoptosis is necessary for intestinal epithelial cell proliferation and repair, but excessive apoptosis increases intestinal permeability and leads to intestinal barrier dysfunction, which in turn induces diarrhea [26, 27]. Our results showed that apoptosis was increased after MPA treatment, and there was no significant change in Bax protein expression, but Bcl-2 protein expression was significantly downregulated, in addition to an increase in activated Caspase 3. In contrast, Sch A upregulated anti-apoptotic protein expression, reduced Caspase 3 activation, and led to a significant decrease in the proportion of apoptotic cells. It indicates that Sch A inhibits MPA-induced apoptosis.

Although Sch A upregulates the expression of TJs and reduces apoptosis to protect intestinal epithelial cells, the mechanism is unclear. It has been reported that the activation of ERK/JNK/p38 MAPK signaling pathway downregulates TJs by increasing ELK1 phosphorylation and inducing the transcription of MLCK [28, 29]; and increases apoptosis through the mitochondrial pathway [30, 31]. And studies have confirmed that MPA regulates TJs through p38 MAPK [10]. Therefore, we then investigated the regulatory role of Sch A on the ERK/JNK/p38 MAPK signaling pathway. By in vitro Western blot experiments, we found that the regulation of the ERK/JNK/p38 MAPK signaling pathway by Sch A was evident, the expression of p-ERK, p-JNK and p-p38 were significantly down-regulated.

It has been confirmed that the increase of reactive oxygen species (ROS) mediated by oxidative stress in intestinal epithelial cells is the key factor which lead to intestinal epithelial cell apoptosis and down-regulation of TJs expression[32, 33]. Arsenite-induced downregulation of occludin in BEAS-2B cells via the

ROS/ERK/ MLCK and ROS/p38 MAPK signaling pathways [9];ROS activates ERK1/2/MLCK pathway to result in endothelial cell tight junction deficiency and barrier dysfunction, leading to acute lung injury and death in CLP-induced septic mice [34]; Vitamin K2 induces mitochondria-related apoptosis in human bladder cancer cells via ROS and JNK/p38 MAPK Signal Pathways [35]. It is suggested that ROS may impair TJs and induce mitochondria-associated apoptosis through activation of the ERK/JNK/p38 pathway. It was found that high concentration of mycophenolate mofetil (MMF) induced oxidative damage that lead to apoptosis by increasing ROS and MDA levels in HCT116 cells [36]. Several previous experiments have shown that Sch A prevents oxidative stress-induced DNA damage and apoptosis by reducing the production of ROS, and protects the human intestinal cells HT-29 from deoxynivalenol (DON)-induced cytotoxicity by inhibiting the MAPK pathway [16, 37]. Therefore, we speculate that the protective effect of Sch A is related to its antioxidant effect. In this study, MPA significantly increased ROS levels, inhibited SOD activity and increased MDA content significantly in Caco-2 cells, while Sch A treatment effectively reduced ROS levels, restored SOD activity and reduced MDA accumulation.

In summary, our study shows that Sch A plays a protective role against MPA-induced Caco-2 cell injury in vitro, and its protective effect on TJs is mediated, at least in part, by reducing oxidative stress and regulating the ERK/JNK/p38 MAPK signaling pathway. The significance of this experiment is the discovery of the protective effect of Sch A on MPA-induced intestinal cell injury, which provides a new research idea to improve the adverse effects caused by MPA related to intestinal permeability.

Conclusions

Sch A attenuated MPA-induced intestinal injury and reversed the inhibition of MPA on Caco-2 cell viability in an in vitro model. In addition, Sch A was found to inhibit MPA-induced oxidative stress, restore TJs expression and reduce apoptosis, possibly through the MAPK signaling pathway. These results suggest that Sch A may be a protective agent to ameliorate MPA-induced intestinal injury.

Declarations

Acknowledgments and funding

This study was supported by the Natural Science Foundation of Anhui Province Education Department (KJ2019A0247), the First Affiliated Hospital of Anhui Medical University Doctoral Research Funds (BSKY2019009).

Conflict of interest statement

The authors declare that they have no known competing financial interests or personal relationships that could have appeared to influence the work reported in this paper.

Author contributions

Yiyun Deng: Formal analysis, Investigation, Methodology, Writing original draft.

Zhe Zhang: Methodology.

Yuanyuan Hong: Methodology, Software.

Lijuan Feng: Methodology, Software.

Yong Su: Funding acquisition, Writing - review & editing.

Dujuan Xu: Conception and design, Formal analysis, Supervision, Project administration.

Data availability

All data included in this study are available upon request by contacting the corresponding author.

Compliance with Ethical Standards

The authors declare that they have no conflict of interest. All procedures performed in studies involving human participants were in accordance with the ethical standards of the institutional and/or national research committee and with the 1964 Helsinki declaration and its later amendments or comparable ethical standards. This article does not contain any studies with animals performed by any of the authors. Informed consent was obtained from all individual participants included in the study.

References

1. Siebert A, Prejs M, Cholewinski G, Dzierzbicka K (2017) New Analogues of Mycophenolic Acid. Mini Rev Med Chem 17(9):734–745
2. Bunnapradist S, Lentine KL, Burroughs TE, Pinsky BW, Hardinger KL, Brennan DC et al (2006) Mycophenolate mofetil dose reductions and discontinuations after gastrointestinal complications are associated with renal transplant graft failure. Transplantation 82(1):102–107
3. Knoll GA, MacDonald I, Khan A, Van Walraven C (2003) Mycophenolate mofetil dose reduction and the risk of acute rejection after renal transplantation. J Am Soc Nephrol 14(9):2381–2386
4. Takemoto SK, Pinsky BW, Schnitzler MA, Lentine KL, Willoughby LM, Burroughs TE et al (2007) A retrospective analysis of immunosuppression compliance, dose reduction and discontinuation in kidney transplant recipients. Am J Transplant 7(12):2704–2711
5. Xie Y, Zhan X, Tu J, Xu K, Sun X, Liu C et al (2021) Atractylodes oil alleviates diarrhea-predominant irritable bowel syndrome by regulating intestinal inflammation and intestinal barrier via SCF/c-kit and MLCK/MLC2 pathways. J Ethnopharmacol 272:113925
6. Zhao L, Li M, Sun K, Su S, Geng T, Sun H (2020) Hippophae rhamnoides polysaccharides protect IPEC-J2 cells from LPS-induced inflammation, apoptosis and barrier dysfunction in vitro via inhibiting TLR4/NF-kappaB signaling pathway. Int J Biol Macromol 155:1202–1215

7. He Y, Chen J, Zhang Q, Zhang J, Wang L, Chen X et al. α-Chaconine Affects the Apoptosis, Mechanical Barrier Function, and Antioxidant Ability of Mouse Small Intestinal Epithelial Cells. Frontiers in Plant Science. 2021;12
8. Groschwitz KR, Hogan SP (2009) Intestinal barrier function: molecular regulation and disease pathogenesis. J Allergy Clin Immunol 124(1):3–20; quiz 1–2
9. Liu Y, Tang J, Yuan J, Yao C, Hosoi K, Han Y et al (2020) Arsenite-induced downregulation of occludin in mouse lungs and BEAS-2B cells via the ROS/ERK/ELK1/MLCK and ROS/p38 MAPK signaling pathways. Toxicol Lett 332:146–154
10. Khan N, Pantakani DV, Binder L, Qasim M, Asif AR (2015) Immunosuppressant MPA Modulates Tight Junction through Epigenetic Activation of MLCK/MLC-2 Pathway via p38MAPK. Front Physiol 6:381
11. Liang Z, Yuan Z, Guo J, Wu J, Yi J, Deng J et al. Ganoderma lucidum Polysaccharides Prevent Palmitic Acid-Evoked Apoptosis and Autophagy in Intestinal Porcine Epithelial Cell Line via Restoration of Mitochondrial Function and Regulation of MAPK and AMPK/Akt/mTOR Signaling Pathway. Int J Mol Sci. 2019;20(3)
12. Son Y, Cheong YK, Kim NH, Chung HT, Kang DG, Pae HO (2011) Mitogen-Activated Protein Kinases and Reactive Oxygen Species: How Can ROS Activate MAPK Pathways? J Signal Transduct 2011:792639
13. Nash A, Samoylova M, Leuthner T, Zhu M, Lin L, Meyer JN et al (2020) Effects of Immunosuppressive Medications on Mitochondrial Function. J Surg Res 249:50–57
14. Qin XL, Chen X, Wang Y, Xue XP, Wang Y, Li JL et al (2014) In vivo to in vitro effects of six bioactive lignans of Wuzhi tablet (Schisandra sphenanthera extract) on the CYP3A/P-glycoprotein-mediated absorption and metabolism of tacrolimus. Drug Metab Dispos 42(1):193–199
15. Kwon DH, Cha HJ, Choi EO, Leem SH, Kim GY, Moon SK et al (2018) Schisandrin A suppresses lipopolysaccharide-induced inflammation and oxidative stress in RAW 264.7 macrophages by suppressing the NF-kappaB, MAPKs and PI3K/Akt pathways and activating Nrf2/HO-1 signaling. Int J Mol Med 41(1):264–274
16. Wan MLY, Turner PC, Co VA, Wang MF, Amiri KMA, El-Nezami H (2019) Schisandrin A protects intestinal epithelial cells from deoxynivalenol-induced cytotoxicity, oxidative damage and inflammation. Sci Rep 9(1):19173
17. Qasim M, Rahman H, Ahmed R, Oellerich M, Asif AR (2014) Mycophenolic acid mediated disruption of the intestinal epithelial tight junctions. Exp Cell Res 322(2):277–289
18. Song Y, Hu W, Xiao Y, Li Y, Wang X, He W et al (2020) Keratinocyte growth factor ameliorates mycophenolate mofetil-induced intestinal barrier disruption in mice. Mol Immunol 124:61–69
19. Assimakopoulos SF, Dimitropoulou D, Marangos M, Gogos CA (2014) Intestinal barrier dysfunction in HIV infection: pathophysiology, clinical implications and potential therapies. Infection 42(6):951–959
20. Chelakkot C, Ghim J, Ryu SH (2018) Mechanisms regulating intestinal barrier integrity and its pathological implications. Exp Mol Med 50(8):1–9

21. Khan N, Binder L, Pantakani DVK, Asif AR (2017) MPA Modulates Tight Junctions' Permeability via Midkine/PI3K Pathway in Caco-2 Cells: A Possible Mechanism of Leak-Flux Diarrhea in Organ Transplanted Patients. Front Physiol 8:438
22. Al-Sadi R, Khatib K, Guo S, Ye D, Youssef M, Ma T (2011) Occludin regulates macromolecule flux across the intestinal epithelial tight junction barrier. Am J Physiol Gastrointest Liver Physiol 300(6):G1054–G1064
23. Zihni C, Mills C, Matter K, Balda MS (2016) Tight junctions: from simple barriers to multifunctional molecular gates. Nat Rev Mol Cell Biol 17(9):564–580
24. He S, Guo Y, Zhao J, Xu X, Song J, Wang N et al (2019) Ferulic acid protects against heat stress-induced intestinal epithelial barrier dysfunction in IEC-6 cells via the PI3K/Akt-mediated Nrf2/HO-1 signaling pathway. Int J Hyperthermia 35(1):112–121
25. Su L, Nalle SC, Shen L, Turner ES, Singh G, Breskin LA et al (2013) TNFR2 activates MLCK-dependent tight junction dysregulation to cause apoptosis-mediated barrier loss and experimental colitis. Gastroenterology 145(2):407–415
26. Souza HS, Tortori CJ, Castelo-Branco MT, Carvalho AT, Margallo VS, Delgado CF et al (2005) Apoptosis in the intestinal mucosa of patients with inflammatory bowel disease: evidence of altered expression of FasL and perforin cytotoxic pathways. Int J Colorectal Dis 20(3):277–286
27. Dong N, Xu X, Xue C, Wang C, Li X, Bi C et al (2019) Ethyl pyruvate inhibits LPS induced IPEC-J2 inflammation and apoptosis through p38 and ERK1/2 pathways. Cell Cycle 18(20):2614–2628
28. Cremonini E, Daveri E, Mastaloudis A, Adamo AM, Mills D, Kalanetra K et al (2019) Anthocyanins protect the gastrointestinal tract from high fat diet-induced alterations in redox signaling, barrier integrity and dysbiosis. Redox Biol 26:101269
29. Liu Y, Wei H, Tang J, Yuan J, Wu M, Yao C et al (2020) Dysfunction of pulmonary epithelial tight junction induced by silicon dioxide nanoparticles via the ROS/ERK pathway and protein degradation. Chemosphere 255:126954
30. Sui X, Kong N, Ye L, Han W, Zhou J, Zhang Q et al (2014) p38 and JNK MAPK pathways control the balance of apoptosis and autophagy in response to chemotherapeutic agents. Cancer Lett 344(2):174–179
31. Yue J, Lopez JM. Understanding MAPK Signaling Pathways in Apoptosis. Int J Mol Sci. 2020;21(7)
32. Aviello G, Knaus UG (2018) NADPH oxidases and ROS signaling in the gastrointestinal tract. Mucosal Immunol 11(4):1011–1023
33. Zhuang Y, Wu H, Wang X, He J, He S, Yin Y (2019) Resveratrol Attenuates Oxidative Stress-Induced Intestinal Barrier Injury through PI3K/Akt-Mediated Nrf2 Signaling Pathway. Oxid Med Cell Longev 2019:7591840
34. Jiang J, Huang K, Xu S, Garcia JGN, Wang C, Cai H (2020) Targeting NOX4 alleviates sepsis-induced acute lung injury via attenuation of redox-sensitive activation of CaMKII/ERK1/2/MLCK and endothelial cell barrier dysfunction. Redox Biol 36:101638

35. Duan F, Yu Y, Guan R, Xu Z, Liang H, Hong L (2016) Vitamin K2 Induces Mitochondria-Related Apoptosis in Human Bladder Cancer Cells via ROS and JNK/p38 MAPK Signal Pathways. PLoS One 11(8):e0161886
36. Ferjani H, Achour A, Bacha H, Abid S (2015) Tacrolimus and mycophenolate mofetil associations: Induction of oxidative stress or antioxidant effect? Hum Exp Toxicol 34(11):1119–1132
37. Choi YH (2018) Schisandrin A prevents oxidative stress-induced DNA damage and apoptosis by attenuating ROS generation in C2C12 cells. Biomed Pharmacother 106:902–909

Abbreviations

ERK Extracellular regulated kinase

JNK c-Jun N-terminal kinase

MAPK Mitogen-activated protein kinases

MDA Malondialdehyde

MMF Mycophenolate mofetil

MPA Mycophenolic acid

ROS Reactive oxygen species

Sch A Schisandrin A

SOD Superoxide dismutase

TJs Tight junction proteins

Figures

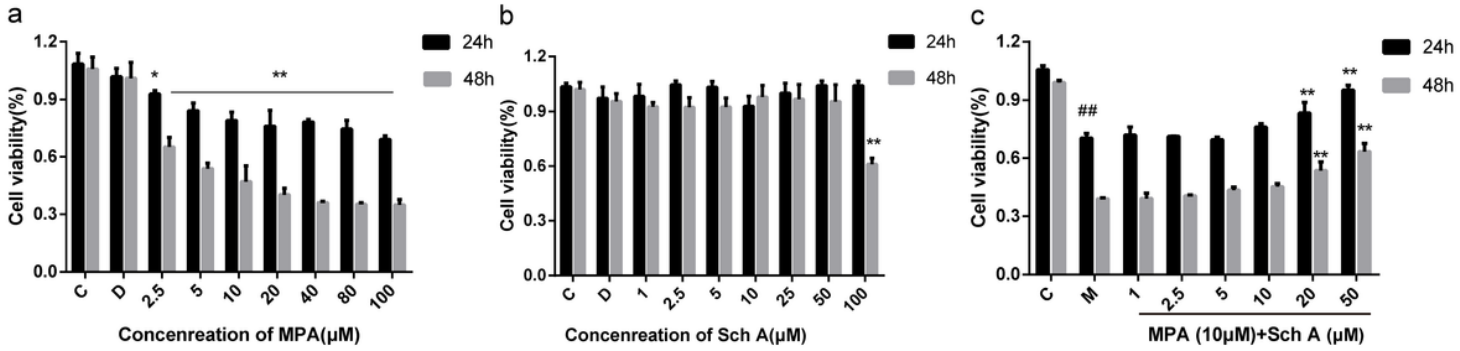

Figure 1

Effect of Sch A on MPA-induced cell viability of Caco-2 cells. Cells were treated with different concentrations of MPA and Sch A for 24h (a, b) and with 10 μM of MPA co-treated with different concentrations of Sch A for 24h (c). Cell viability was detected by MTT assay. The data were presented as mean ± SD, n = 3. *, **P < 0.05 and 0.01 significantly different from MPA treated cells, ##P < 0.01 significantly different from control.

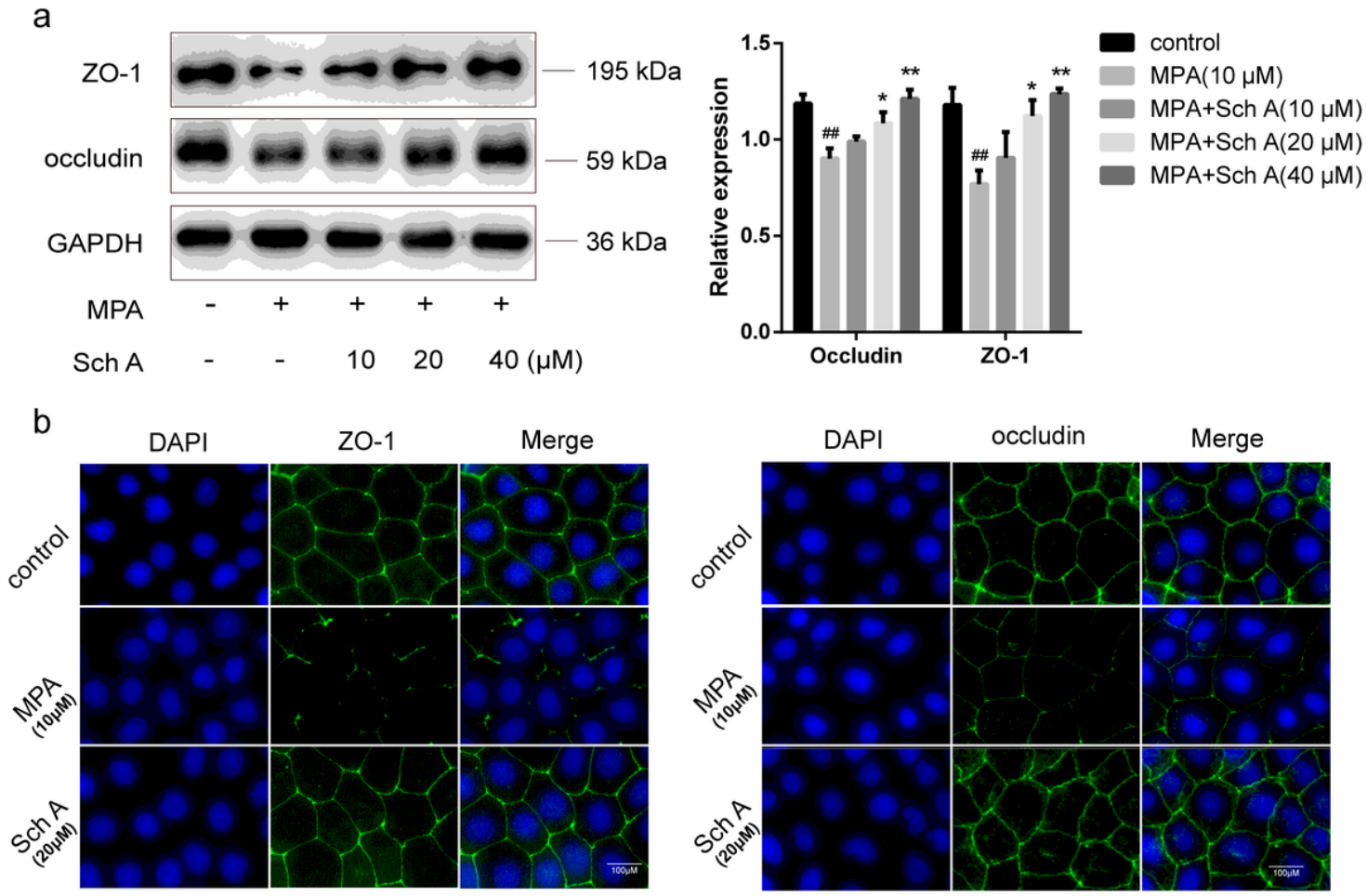

Figure 2

Effect of Sch A on MPA-induced ZO-1 and occludin proteins in Caco-2 cells. Cells were treated with MPA (0/10 μM), MPA (10 μM) + Sch A (10-40 μM) for 24h, and the expression of ZO-1 and occludin proteins in Caco-2 cells was detected by Western Blot (a) and immunofluorescence assay (b). Occludin and ZO-1 showed green fluorescence, and DAPI-stained nuclei showed blue fluorescence. The data were presented as mean ± SD, n = 3. *, **P < 0.05 and 0.01 significantly different from MPA treated cells, ##P < 0.01 significantly different from control. The bar represents 100 μm.

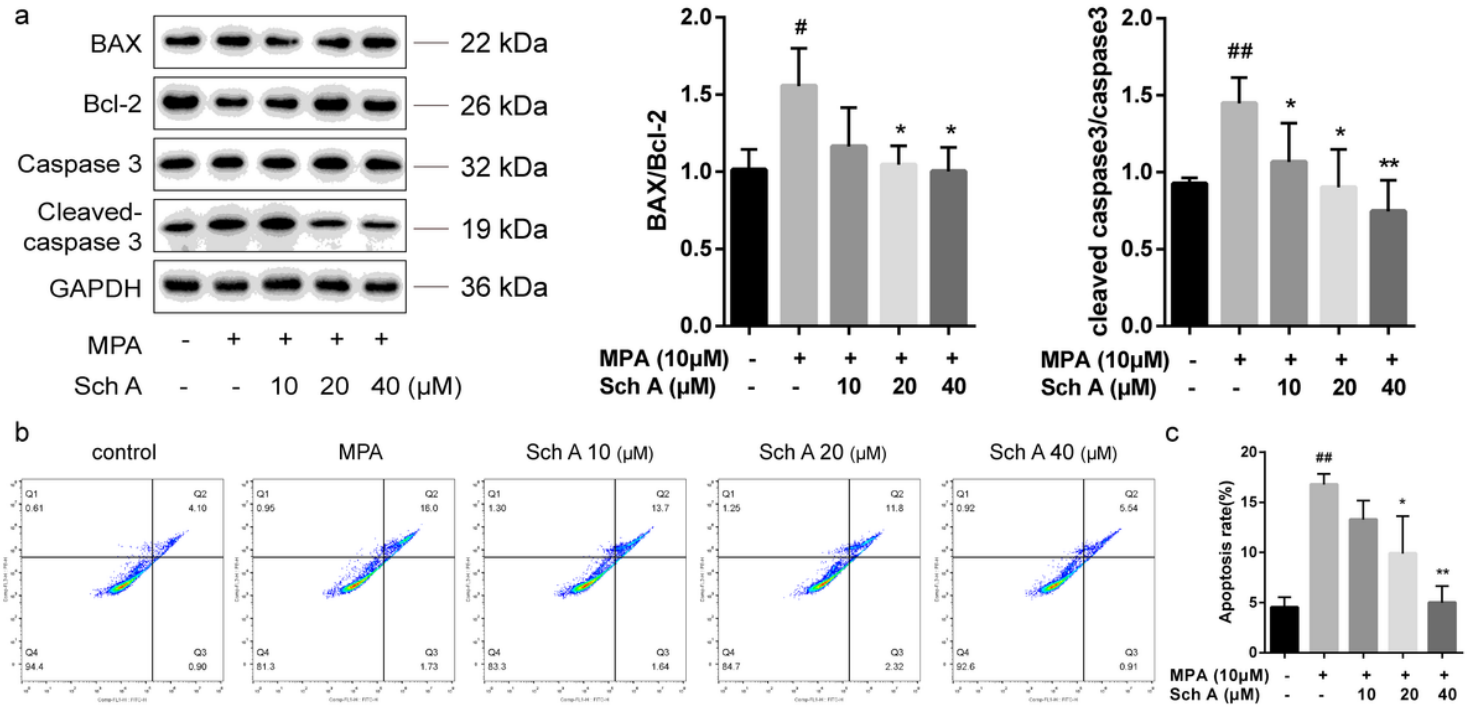

Figure 3

Effect of Sch A on MPA-induced apoptosis in Caco-2 cells. Caco-2 cells were treated with different concentrations of Sch A and MPA (0/10 μM) + Sch A (10-40 μM) for 24h. The expression of Bax/Bcl-2, Cleaved Caspase-3/Caspase-3 in Caco-2 cells was detected by Western Blot (a); apoptosis was detected by flow cytometry after membrane linked protein V-FITC/PI staining (b); (c): quantification of (b). The data were presented as mean ± SD, n = 3. *, **P < 0.05 and 0.01 significantly different from MPA treated cells, #, ##P < 0.05 and 0.01 significantly different from control.

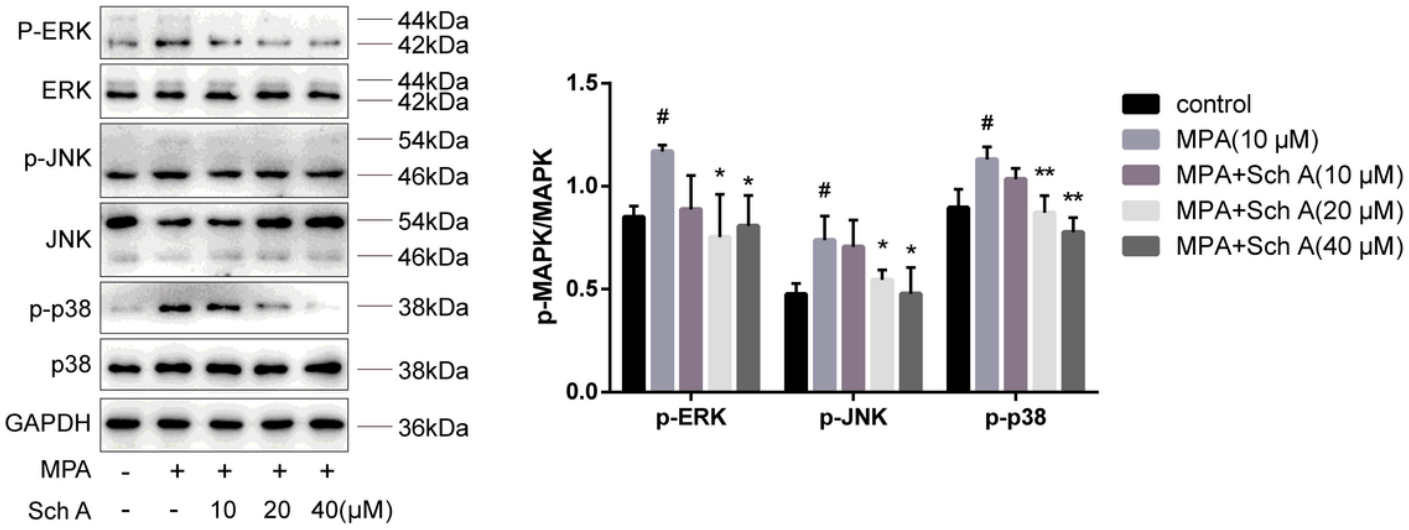

Figure 4

Sch A inhibits MPA-induced activation of the ERK/JNK/p38 MAPK signaling pathway. Caco-2 cells were treated with different concentrations of Sch A and MPA (0/10 μM) for 24 h. The total ERK/JNK/p38 levels and phosphorylation levels in Caco-2 cells were measured by Western Blot. *, **P < 0.05 and 0.01 significantly different from MPA treated cells, #P < 0.05 significantly different from control.

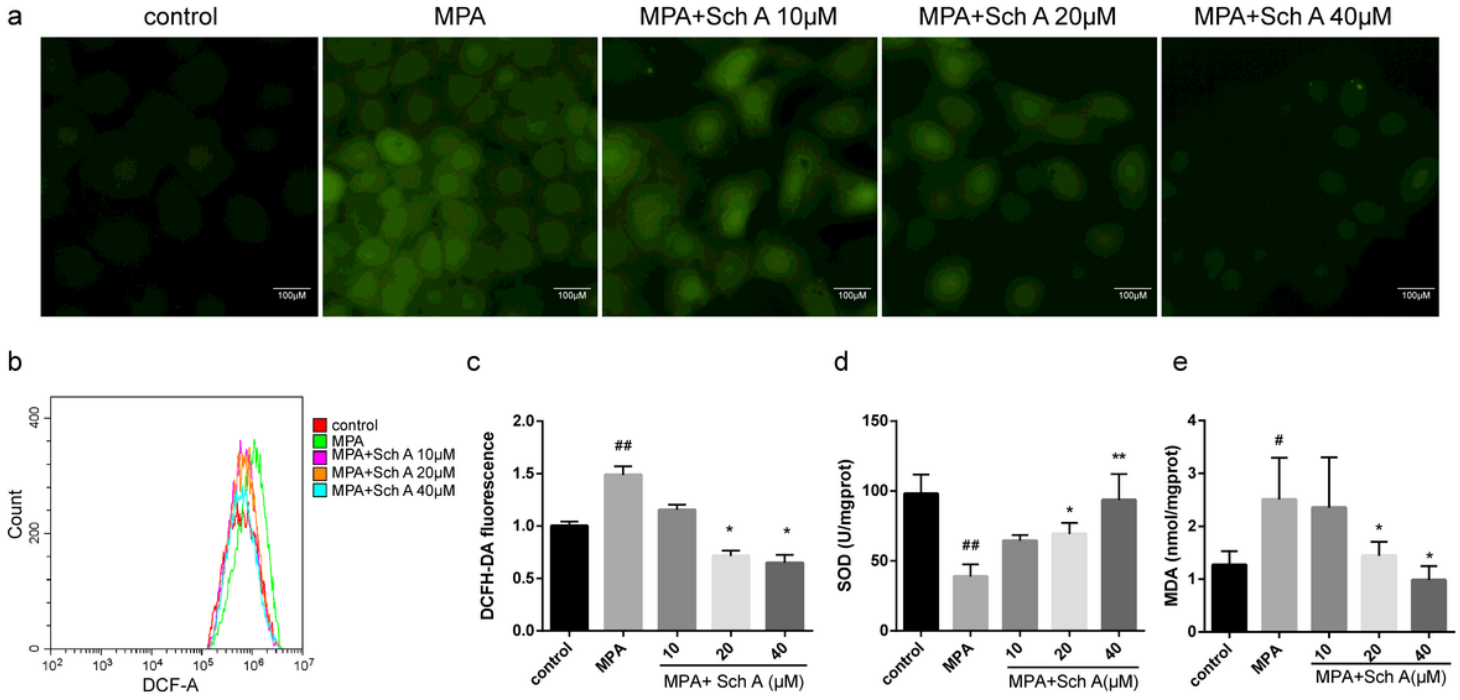

Figure 5

Effect of Sch A on MPA-induced oxidative stress in Caco-2 cells. Caco-2 cells were treated with different concentrations of Sch A and MPA (0/10 μM). Fluorescence microscopy to detect ROS in cells treated with H2DCF-DA probe (a); flow cytometry to detect ROS production (b, c); SOD activity (d); MDA content (e). The data were presented as mean ± SD, n = 3. *, **P < 0.05 and 0.01 significantly different from MPA treated cells, #, ##P < 0.05 and 0.01 significantly different from control. The bar represents 100 μm.

Supplementary Files

This is a list of supplementary files associated with this preprint. Click to download.

- FlowcytometryApoptosis.tif
- FlowcytometryROS.tif
- Immunofluorescenceoccludinfitc.tif
- Immunofluorescenceoccludinmerge.tif
- Immunofluorescencezo1fitc.tif

- Immunofluorescencezo1merge.tif
- MTT.xlsx
- ROSFluorescence.tif
- SODMDA.xlsx
- WBApoptosis.tif
- WBMAPK.tif
- WBTJs.tif